MECHANICAL PROPERTIES AND PROCESS FORCES DURING FRICTION STIR WELDING OF AA2219 AT VARIABLE WELDING SPEED AND TOOL ROTATION

Kanwer Singh Arora

Research and Development, Tata Steel Limited, Jamshedpur - 831001

ABSTRACT - *Welding speed and tool rotation (rpm) were varied systematically during friction stir welding of aluminium alloy 2219-T87. The effect of these parameter on process forces and mechanical properties of the weld joints was studied. It was observed that increasing welding speed resulted in higher process forces due to decrease in heat input whereas inverse relation between tool rotations and process forces was recorded. Weld nugget was observed to consist of fine equiaxed grains probably due to continuous dynamic recrystallization due to heat and shear deformation as a result of stirring of material.*

Introduction

Friction stir welding (FSW) was developed and patented by The Welding Institute (TWI, Cambridge, UK) in 1991 [1]. It is a solid state joining process, which utilizes a rotating cylindrical tool of high strength material. The tool goes into the abutting edges of two firmly clamped work plates and travels along the edges stirring the material together and formation of the joint. Optimized parameters result in defect free joints forged at temperature much below the melting point of the joined material [2-4]. Weld nugget is the region approximately the same width as pin diameter ad consist of recrystallized grains. On either side of the nugget thermo mechanically affect zone (TMAZ) and heat affected zone (HAZ) are formed.

Experimental Procedure

In this study friction stir welding of 5 mm thick AA2219-T87 alloy was carried out using a conventional milling machine. . AA2219-T87 is a high strength precipitation hardened Al–Cu alloy ad posses the precipitation aging sequence of $\alpha \rightarrow \alpha + $ GP Zones $\rightarrow \alpha + \theta'' \rightarrow \alpha + \theta' \rightarrow \alpha + \theta$. Here aluminium solid solution is defined as α, observed metastable phases are denoted as θ', θ'' and the stable precipitates are represented by θ [5]. This alloy is used i aerospace ad space industries as it displaces good mechanical properties over a wide temperature range of 250 to -250 ºC. Mechanical properties of this alloy is listed in Table 1.

Table1: Mechanical properties of Base Material

Tensile Strength (MPa)	Yield Strength (MPa)	Elongation at fracture (%)	Vickers Hardness	Average Grain Length
460±15	370±10	13±1 %	145± 5HV0.1	25±2 μm

Friction stir welding was achieved by joining two AA2219 plates each measuring 200 x 50 x 5 mm3. The tool was titled backward at an angle of 2° , this has shown to help achieve defcet free weld joints. A steel backing plate was kept below the material to be joined. Both AA2219 and steel plate were firmly clamped onto the upper plate of a designed and fabricated load measuring fixture (Fig. 1). Clamping is necessary to avoid openng up of the abutting edges on tool penetration and traverse. The load measuring fixture was able to measure both Z-direction (forging) and X-direction(welding) forces.
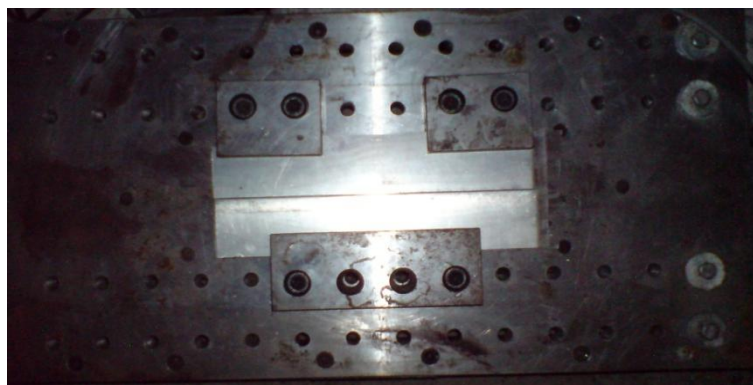

Fig. 1: AA2219 plates clamped on the load measuring fixture

This article discusses effect of welding speed and tool rotation variations (Table 2). Tool dimensions (shoulder diameter and pin diameter) and geometry (pin profile) were not varied.. Weld length of 150-175 mm was achieved for the welds. One such joint in shown in Fig. 2.

Table 2: Weld Parameters

Sample No.	Weld Designation	Welding Speed (mm/min)	Shoulder diameter (mm)	Pin diameter (mm)	RPM
1	CS1	45	20	8	250
2	CS2	90	20	8	250
3	CS3	135	20	8	250
4	CR1	90	20	8	200
5	CR2	90	20	8	300

Fig. 2: FSW tool profile

Results & discussion

Forces
Increase in welding speed resulted in proportional increase in forging and welding direction forces (for constant rpm value). This can be attributed to increased volume of material encountered by the tool pin per unit time. Whereas, tool rpm inversely affected the force values because heat generated by tool rpm (for the selected rpm range) reduces the strength f the material by dissolution of precipitates. The recorded forces are listed in Table 3 and graphical representation of the same is shown in Fig. 3.

Table 3: Force values for the three weld parameters combination

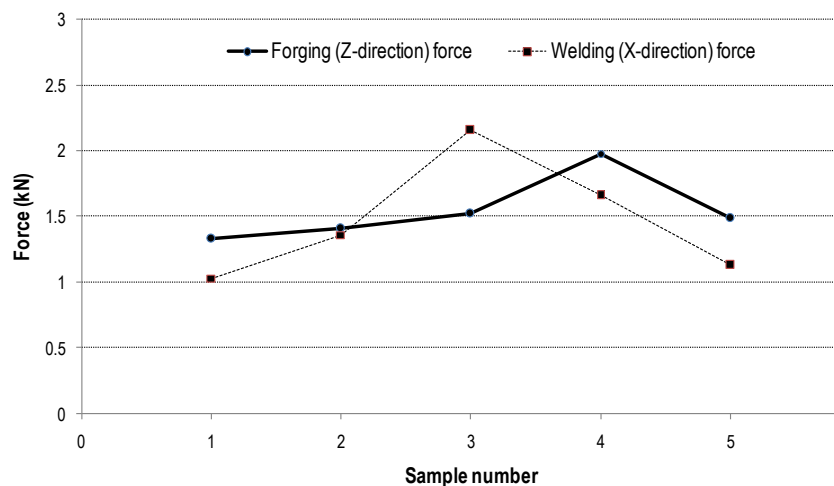| Sample No.	Sample Designation	Maximum value of Forces	
		Z-direction-forging force (kN)	X-direction-welding force (kN)
1	CS1	1.33	1.03
2	CS2	1.41	1.36
3	CS3	1.52	2.16
4	CR1	1.98	1.66
5	CR2	1.49	1.13

Fig. 3: Variation of Process forces

Microstructure

Microstructure analysis of the weld was carried out by polishing samples sectioned transverse to the welding direction. The samples were polished according to standard metallography practice and etched using Keller's reagent at room temperature. Fig. 4(A) shows the microstructure of the parent material. Fig. 4(b) shows the macro-image of the friction stir weld. Whereas, the weld nugget in shown in Fig. 4(c) and Fig. 4d) shows the TMAZ and HAZ regions. Weld nugget consists of recrystallized equiaxed grains, with the grain size decreasing from the top to bottom surface, which could be a result of chilling effect of backing plate as against the rotating tool pin which generated heat at the top surface. The rotating tool causes both heat generation and shear deformation in the weld nugget, which facilitates continuous dynamic recrystallization causing grain refinement.

Hardness

Vickers hardness measurement was carried out using 100gf and 15s dwell time, across the weld along the mid-thickness. Fig. 5 shows the hardness profile. The distance between indent was kept as 250μm. as per ASTM E384 recommendations. Vickers hardness profile is inverted U-shaped one indicating minimum hardness in the weld nugget. the hardness continuously increases to parent material value as we move away from the weld nugget.
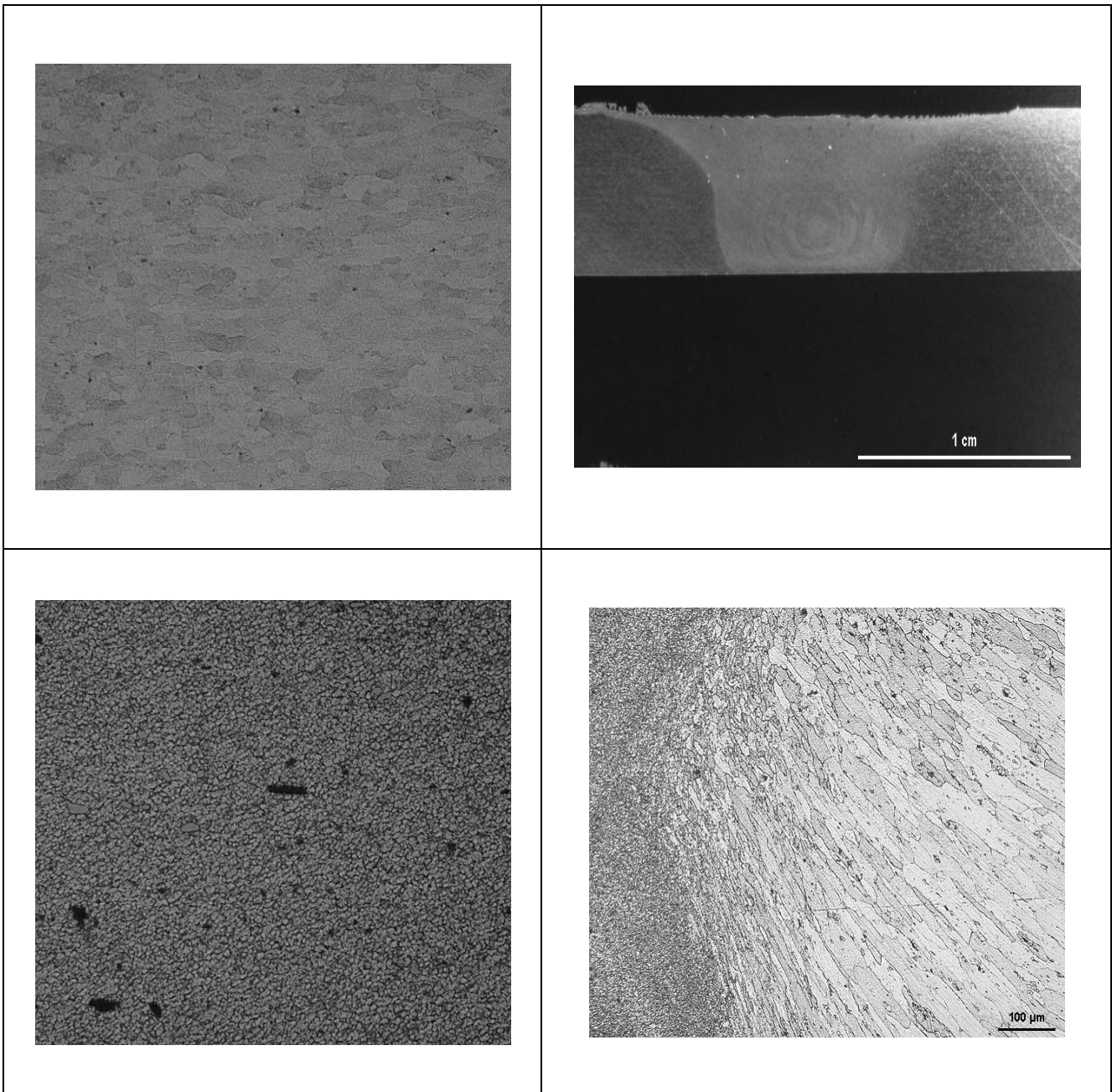

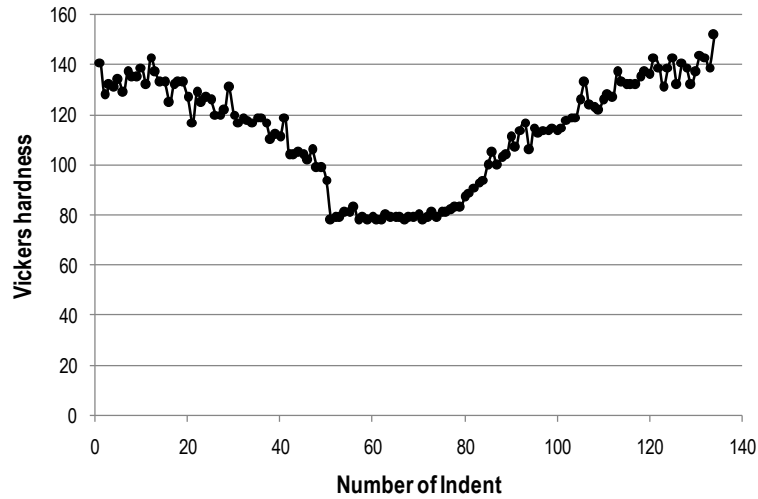Fig. 4: (a) Parent material microstructure (b) Macro image of weld (c) Weld nugget and (d) TMAZ and HAZ regions

Fig. 5 : Vickers microhardness profile across weld zone

Tensile Tests

Three subsize tensile specimen with a parallel length of 32 mm were machined transverse to the welding direction for each of the joints. as per ASTM E8 standard. Tensile test were carried out using a Zwick-Roell tensile testing machine of 100 kN capacity. The decrease in the softening of the weld with increasing welding speed, also observed in hardness measurements, results in increase in the strength of the welds. A maximum joint efficiency of 67% was observed for weld fabricated at welding speed of 135 mm/min and tool rpm 250 as reported in Table 4.

Table 4: Tensile test results of weld joints

Weld Designation	Yield strength (N/mm^2)	UTS (N/mm^2)	% elongation	Joint efficiency %
A	170±12	260±10	15±2	61
B	175±15	280±15	15±1	65
C	190±10	300±10	14±2	67
	160±12	260±15	13±2	60
	150±20	250±20	12±3	58

Fractography

Tensile test surface were observed in a scanning electron microscope to understand the fracture characteristics. The welds failed in a typical ductile manner with the fracture showing dimples (Fig. 6), which are formed a s a result of micro-void coalescences. Also, inclusion were observed in few fracture surfaces and it can be safely concluded that these are coarsened Al2Cu particle. No external inclusions can be observed since friction stir welding is a solid state joining process [6]
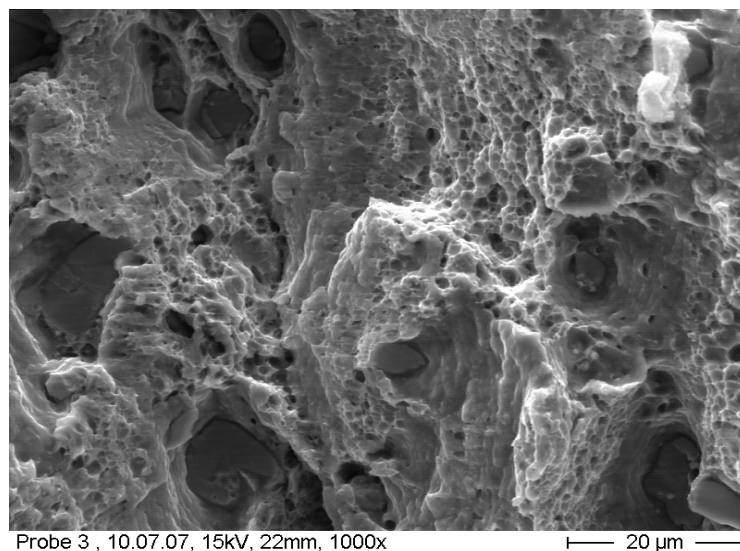

Probe 3 , 10.07.07, 15kV, 22mm, 1000x   20 µm
Fig. 6: Fracture surface

Conclusions

1. Friction stir welding of high strength aluminium alloy 2219-T87 was successfully conducted using friction stir welding by varying welding speed and tool rotations per minute.
2. Tensile strength and hardness of the joint was observed to increase with increasing welding speed.
3. Process forces varied proportionally with increasing welding speed and inversely when tool rotation per minutes were increased.
4. Weld nugget consisted of very fine equiaxed grains caused by combined effect of heat and shear deformation.
5. minimum hardness was observed in the weld nugget and the drop in nugget hardness was proportional to heat input during welding.

References

1 M. Guerra, C. Schmidt, J.C. McClure, L.E Murr, and A.C.Nunes, Flow patterns during friction stir welding, Materials Characterization, Volume 49, Issue 2, 2002, pp. 95-1012.
2. M.A. Sutton, B. Yang, A. P. Reynolds and R. Taylor, Microstructural studies of friction stir welds in 2024-T3 aluminium", Materials Science and Engineering A, 2002; Vol. 323: pp. 160-166.
3.. B. Yang, J. Yan, M. A. Sutton and A. P. Reynolds, Banded microstructure in AA2024-T351 and AA2524-T351 aluminium friction stir welds, Part I. Metallurgical studies, Material Science and Engineering A 2004; Vol. 364: pp. 55-56.
4. H.J. Liu, H. Fuji, M. Maeda and K. Nogi, Tensile properties and fracture locations of friction-stir-welded joints of 2017-T351 aluminum alloy, Journal of Materials Processing Technology, Volume 142, Issue 3, 2003, pp. 692-6965.
5. J. M. Papazian, A calorimetric study of precipitation in aluminum alloy 2219, Metallurgical Transactions A, Volume 12, Issue 2, 1981, pp 269–280
6 G. Cao and S. Kou Friction Stir Welding of 2219 Aluminium: Behaviour of θ (Al2Cu) particles, Welding Journal, 2005; pp. 1s-8s.